Fast pixel shifting phase unwrapping algorithm in quantitative interferometric microscopy

Liang Xue (薛 亮)[1+*], Shouyu Wang (王绶玙)[2,3+], Keding Yan (闫克丁)[2,4], Nan Sun (孙 楠)[5], Zhenhua Li (李振华)[2], and Fei Liu(刘 斐)[3]**

[1] *College of Electronics and Information Engineering, Shanghai University of Electric Power, Shanghai 200090, China*

[2] *Department of Information Physics and Engineering, Nanjing University of Science and Technology, Nanjing 210094, China*

[3] *Single Molecule Nanometry Laboratory, College of Veterinary Medicine, Nanjing Agricultural University, Nanjing 210095, China*

[4] *School of Electronic Information Engineering, Xi'an Technological University, Xi'an 710032, China*

[5] *Institute of Quality Inspection of Electronics and Electrical Appliances, Shanghai Institute of Quality Inspection and Technical Research, Shanghai 201114, China*

[+] *These authors contributed equally to this work*

[*] *Corresponding author: xueliangokay@gmail.com;* [**] *corresponding author: feiliu24@njau.edu.cn*

Received January 2, 2014; accepted April 4, 2014; posted online June 20, 2014

Quantitative interferometric microscopy is an important method for observing biological samples such as cells and tissues. As a key step in phase recovery, a fast phase unwrapping algorithm is proposed. By shifting mod 2π wrapped phase map for one pixel, then multiplying the original phase map and the shifted one, the phase discontinuities could be easily determined with high speed and efficiency. The method aims at enhancing phase retrieving efficiency without any background knowledge. We test our algorithm with both numerical simulation and experiments, by focusing our attentions on wrapped quantitative phase maps of cells. The results indicate that this algorithm features fast, precise and reliable.

OCIS codes: 180.3170, 120.5050.
doi: 10.3788/COL201412.071801.

Optical microscopy[1,2] is a fast developing technique in last decades since it promotes interdisciplinary research in biological and medical sciences. Most biological cells, including red blood cells (RBCs) and HeLa cells, are nearly transparent under visible-light illumination and behave essentially as phase objects. To quantitatively obtain the phase image of the biological cells, two types of phase imaging are often used. One is noninterferometric phase imaging[3,4] while the other is quantitative interferometric microscopy (QIM)[5]. In order to obtain phase distribution of the sample, phase extraction and phase unwrapping are needed in QIM. There is a wealth of phase extraction algorithms, such as phase shifting methods[6], principal component analysis (PCA)[7−9], fast Fourier transform method (FFT)[10,11], Hilbert transform method (HT)[12−16], spatial phase-shifting algorithm[17,18] and derivative algorithm[19], etc. After phase extracting, the solved phase distributions are always wrapped from $-\pi$ to π caused by tangent function in the situation of thick phase samples or off-axis interferometry setup. Phase unwrapping is used to eliminate the ramps to achieve continuous phase distributions. There are also many phase unwrapping algorithms, but some of these methods such as least squares algorithm[20], minimum network flow method[21], etc. are time-consuming to locate the phase discontinuities which leads to low processing efficiency. Besides, some high-speed phase unwrapping methods have been proposed. Kim *et al.* used two interferograms captured at two different wavelengths to obtain the unwrapped phase distributions[22]. While this method could not eliminate all the wraps in the phase fields as the difference of these two wavelengths is obvious or the field of view (FOV) is large where there are too many wraps. Pham *et al.* developed a non-phase wrapping white light diffraction phase microscopy by capturing one interferogram with biological samples and another interferogram without samples as background[23]. Though this method simplifies the phase retrieving process, however, the phase of the tested samples could not exceed 2π and it is difficult to obtain the accurate phase distribution if the sample is located in the position of phase discontinuities. Nevertheless, both methods need at least two interferograms to recover final phase distributions. The limitation hinders the developments of real-time QIM. Moreover, much fast speed phase unwrapping methods have been proposed[24,25], however, some of them need much complicated procedures which increase the difficulty of such algorithms.

In this letter, we have proposed a fast phase unwrapping algorithm to realize high-speed QIM in low noise condition. The new-designing high-speed pixel shifting phase unwrapping algorithm, combined with phase extraction methods, could be applied to recover the continuous phase distributions of the biological samples. Compared to traditional phase unwrapping methods, this method has high calculating efficiency and easy procedures.

Phase extraction includes FFT method[10,11], HT method[12−16], etc., almost all of which are rapid methods. However, most phase unwrapping methods are quite

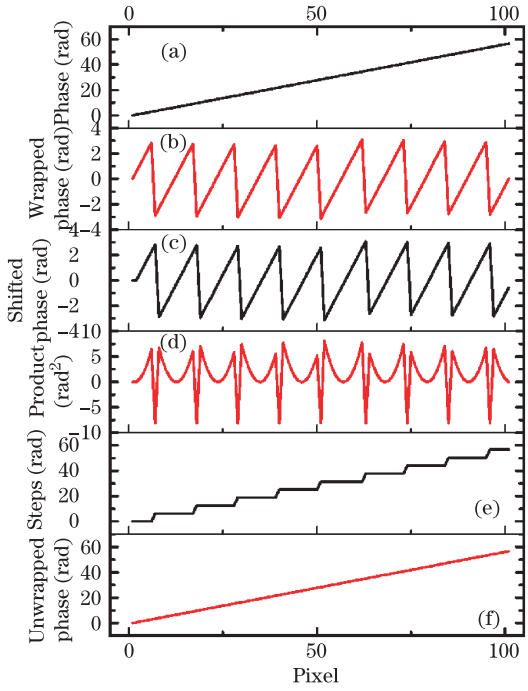

Fig. 1. Simulation of phase unwrapping algorithm. (a) Phase of an inclined plane in simulation; (b) wrapped phase distribution after phase extraction; (c) shifted wrapped phase distribution of (b) with one pixel to the right; (d) multiplication of wrapped phase distribution (b) and shifted wrapped phase distribution (c); (e) phase steps obtained from (d); (f) unwrapped phase distribution.

time-consuming in the whole phase reconstruction procedure, so high-speed phase unwrapping algorithm is required to improve the calculation efficiency. Here, we propose a fast phase unwrapping algorithm to realize high-speed QIM. The basic principle of new phase unwrapping is described in Fig. 1, which illustrates the numerical values used in generating the simulation plots. Suppose the object is an inclined plane with a phase height of 18π shown as in Fig. 1(a). In the first step-phase extraction, the wrapped phase distribution in a range of $[-\pi, \pi)$ will be obtained as Fig 1(b); in the second step-phase unwrapping, firstly, the solved wrapped phase is shifted by one pixel to the right as Fig. 1(c). Next, if we multiply the original wrapped phase distribution with the shifted one, the multiplication result is shown as Fig. 1(d). It is not difficult to see at phase discontinuities, the products are relatively large negative values and close to $-\pi^2$ due to a relatively large negative phase value ($\sim -\pi$) and a relatively large positive phase value ($\sim \pi$) at the phase discontinuity. As a result, the positions of large negative values are where the phase discontinuities locate. Finally, after finding the phase discontinuities, the steps of phases could be obtained as Fig. 1(e) according to Fig. 1(d) and phase jumping direction obtained by phase wrapped information, then the continuous phase distributions could be obtained by adding wrapped phase and phase steps, which are given in Fig. 1(f). This new phase unwrapping algorithm only needs single interferogram without any background information or dual wavelength images.

This new phase unwrapping approach has several advantages. Firstly, compared with traditional path dependent phase unwrapping, the new method has a wide range of $[-\pi^2, \pi^2)$ which is larger than $\sim[0, 2\pi)$ of traditional methods. Figure 2(a) is the phase discontinuity determination of traditional path dependent phase unwrapping method calculated from Fig. 1(b), it is obtained by adjacent point subtraction. The range of the result is in a range of $\sim[0, 2\pi)$. The peak values indicate there are phase discontinuities. Figure 2(b) is obtained from Figs. 1(b) and (c), which applies the proposed method to determine the phase discontinuities. The range of the result is in a range of $[-\pi^2, \pi^2)$. As seen in Figs. 2(a) and (b), the large range is helpful for distinguish the phase discontinuities. Figure 2(c) demonstrates the wrapped phase with low noise consideration. The results in Figs. 2(c) and (d) clearly show the method works well. Moreover, phase discontinuities could not only be determined by the negative relative large value, but it is also much easier to determine the phase discontinuities since the phase discontinuities are between two extreme values. These features will help to find the real phase discontinuities from bumps introduced by noise. Figure 2(e) shows the wrapped phase distribution with bumps. With traditional methods, these bumps may be treated as phase discontinuities that induce errors as Fig. 2(f). While applying this proposed phase wrapping method, there will exist some negative values but they are not between two extreme values so these bumps could be distinguished from phase discontinuities as Fig. 2(g). As a result, even under noise conditions, the proposed phase unwrapping method could recover continuous phase distributions with high calculating efficiency and accuracy.

However, in the occasion of large noise, by applying this method, there will be several continuous negative values in multiplication result between two relative high positive values, which will be difficult to determine the accurate positions of phase discontinuities. Moreover, too large noise sometimes will make the absolute number of the negative values in multiplication result not so large. Since phase discontinuities are determined through setting threshold, which will lead to phase discontinuity missing. Therefore, the method only work well and

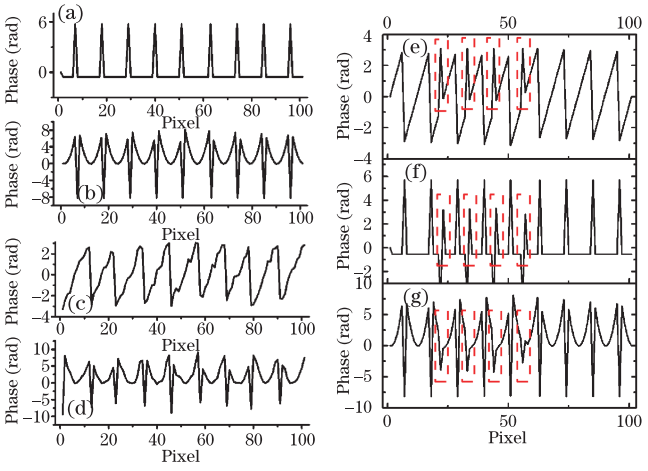

Fig. 2. Simulation of phase unwrapping algorithm. (a) Traditional path dependent phase unwrapping method, phase difference between adjacent points; (b) proposed phase unwrapping method as Fig. 1(d); (c) wrapped phase with noise; (d) proposed phase unwrapping method as Fig. 1(d); (e) wrapped phase with bumps; (f) traditional path dependent phase unwrapping method; (g) proposed phase unwrapping method.

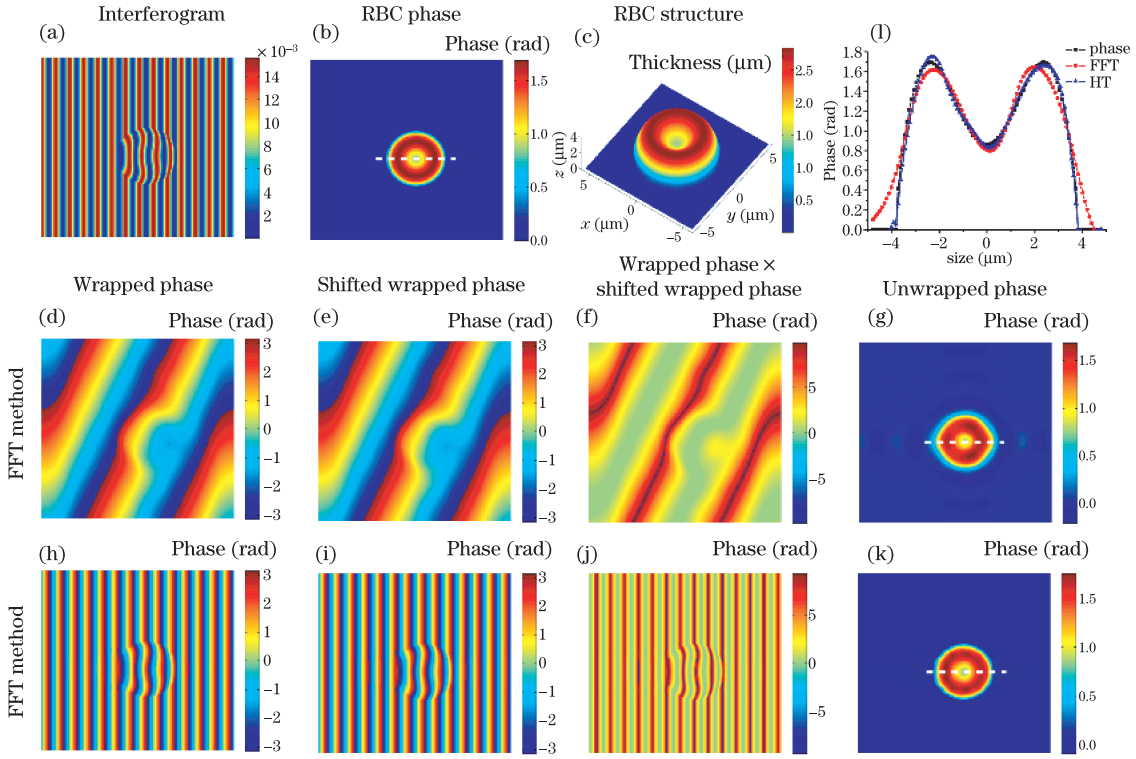

Fig. 3. Simulation of high-speed QIM. (a) interferogram; (b) phase distribution of RBC model; (c) structure of RBC model; (d) wrapped phase distribution retrieved by FFT method; (e) one pixel rightwards shifted wrapped phase map of (d); (f) multiplication of (d) and (e); (g) continuous unwrapped phase distribution by FFT method; (h) wrapped phase distribution retrieved by HT method; (i) one pixel rightwards shifted wrapped phase distribution of (h); (j) multiplication of (h) and (i); (k) continuous unwrapped phase distribution by HT method. (l) section comparisons along white lines in (b)-black, (g)-red and (k)-blue.

correctly in low noise conditions. From the theory and analysis, we have shown that the fast phase unwrapping method based on pixel shifting could work well in low noise condition. In the following part, we will apply this method in QIM in order to quantitatively retrieve the phase distribution of RBCs at different noise levels. In order to show the feasibility of new approach in high-speed QIM, here, we have demonstrated the simulation as shown in Fig. 3.

Figure 3(a) is an off-axis interferogram and the detected phase model is a RBC. Mature RBCs are biconcave disks. They lack cell nucleus and most organelles. The RBCs' cytoplasm is rich in hemoglobin. Since the structure of RBC is almost uniform, therefore, many researches treat RBC as the homogeneous object. The following formula describes the RBC with concave shape[26]:

$$z(\rho) = \left[1 - \left(\frac{\rho}{a}\right)^2\right]^{1/2}\left[0.72 + 4.152\left(\frac{\rho}{a}\right)^2 - 3.426\left(\frac{\rho}{a}\right)^4\right]. \quad (1)$$

The model is a statistical result from experimental observation which shows an average-sized RBC in an isotonic saline solution. The RBC behaves a biconcave disk and the axisymmetric geometry could be described analytically on the ρ–z plane of a cylindrical coordinate system. According to the statistical results, RBC has a diameter of $2a$=7.65 μm, a maximum and a minimum thickness of 2.84 and 1.44 μm, respectively. The RBC is homogeneous so that the refractive index is set as ~1.4. The phase difference could be calculated by

$$\Delta\varphi = \Delta n \cdot L/\lambda, \quad (2)$$

Δn is refractive index difference between RBC model and surrounding solution (0.9% mass fraction NaCl solution with refractive index ~1.34), L is the thickness of the RBC model and λ is the wavelength that is 632.8 nm in both simulation and experiment. Figure 3(b) shows the phase distribution of RBC model and Fig. 3(c) is the structure of RBC model. The second and third rows show the results of different phase extraction methods, FFT and HT, respectively. Figure 3(d) is the wrapped phase distribution solved by FFT method. Compared with Fig. 3(d), Fig. 3(e) is the shifted wrapped phase distribution with one pixel rightwards. Figure 3(f) is the multiplication of wrapped phase distribution and shifted wrapped phase distribution. From Fig. 3(f), it is clear to see the lines (in blue) passing through relative large negative values divide the wrapped phase into several parts. Applying the theory of the fast phase unwrapping method, Fig. 3(g) could be obtained after cancelling the tilting phase backgrounds. The high speed phase unwrapping method could also be combined with HT phase extraction method. The process is represented in Figs. 3(h)−(k) corresponding to the figures of FFT method. Figures 3(g) and (k) are phase retrieval results obtained from FFT and HT methods, respectively. The solved structure is close to the set phase distribution of Fig. 3(b). We have adopted correlation coefficient (*c.c.*) to

evaluate the solved results and the set phase distribution in simulation. The explanation of *c.c.* is shown as

$$c.c. = \frac{\sum_m \sum_n (A_{mn} - A_{\text{ave}})(B_{mn} - B_{\text{ave}})}{\sqrt{\sum_m \sum_n (A_{mn} - A_{\text{ave}})^2 \sum_m \sum_n (B_{mn} - B_{\text{ave}})^2}}, \quad (3)$$

where A is the original set phase distribution, and B is the phase distribution solved by phase retrieval algorithm. Both phase distributions occupy the same the area which is m by n. A_{ave} and B_{ave} are the mean values of A and B, respectively.

The *c.c.* between solved phase distribution by fast phase retrieval method with FFT method and set phase distribution is 0.9846; and *c.c.* between solved phase distribution by fast phase retrieval method with HT method and set phase distribution is 0.9990. The value of both *c.c.*'s are quite close to 1 illustrating the fast phase retrieval method has a high accuracy. Because the HT phase extraction method remains more high order information than FFT method in frequency domain, so it keeps more details of the phase. Moreover, we compare sections of RBCs in our simulation results as shown in Fig. 3(l). The results show clearly that retrieval results match well with the original setting phase. Besides, we have also calculated the time consuming of different phase unwrapping method with single interferogram. The wrapped phase distribution with a size of 256×256 pixels is calculated by computer with Intel Core i5 CPU M520 at 2.40 GHz with 4 GB RAM. Each algorithm is executed many times and Table 1 reports the average execution time. The proposed method in this letter only needs 6.723 ms and it is fastest among three algorithms, while the old version of phase unwrapping methods used by our research group need 3.718 s (two-dimensional (2D) unweighted least squares algorithm based on the discrete cosine transform[20]) and 5.919 s (2D unwrapping based on Minimum Network Flow[21]) in realizing phase unwrapping, respectively. This new rapid phase retrieval method runs much faster than that of the conventional phase unwrapping algorithms which could significantly improve the calculating efficiency and with this method, real time monitoring and detecting as well as large scale phase distribution data analysis of biological samples could be realized.

Moreover, we do the simulation considering the effect of Gaussian noise. The interferogram with low noise is shown in Fig. 4(a). The signal-to-noise ratio (SNR) of the interferogram is ∼40 dB, which is a low noise occasion. Figures 4(b) and (c) are retrieved phase distributions of the RBC model from interferogram by FFT and HT method with minimum network flow phase unwrapping method, respectively. The *c.c.* of these phase

Table 1. Comparisons of Phase Unwrapping Time for Different Algorithms for 256×256 Array Size on a Personal Computer (Intel Core i5 CPU M520 at 2.40 GHz with 4 GB RAM)

Data Algorithm	Time Consuming
Proposed Method	6.723 ms
Least Squares Algorithm[20]	3.718 s
Minimum Network Flow[21]	5.919 s

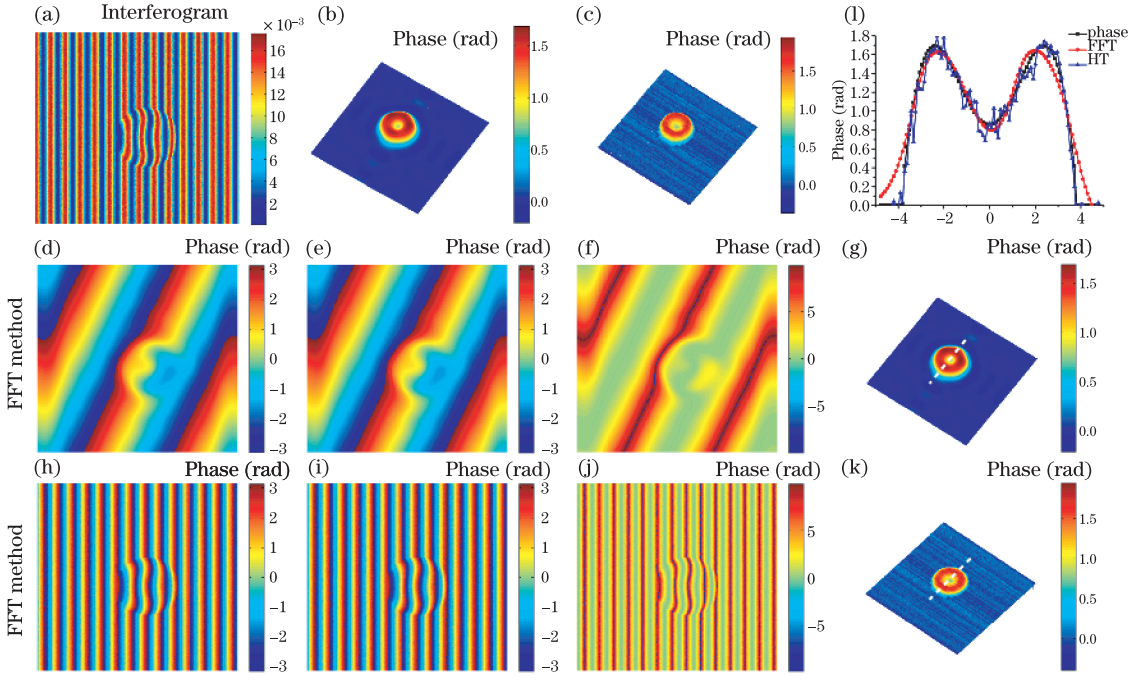

Fig. 4. Simulation of interferogram with noise. (a) Interferogram with noise; (b) phase distribution of RBC model by FFT method with minimum network flow phase unwrapping method; (c) phase distribution of RBC model by HT method with minimum network flow phase unwrapping method; (d) wrapped phase distribution retrieved by FFT method; (e) one pixel rightwards shifted wrapped phase map of (d); (f) multiplication of (d) and (e); (g) continuous unwrapped phase distribution by FFT method; (h) wrapped phase distribution retrieved by HT method; (i) one pixel rightwards shifted wrapped phase distribution of (h); (j) multiplication of (h) and (i); (k) continuous unwrapped phase distribution by HT method. (l) section comparison along white lines in Fig. 3(b)-black, (g)-red and (k)-blue.

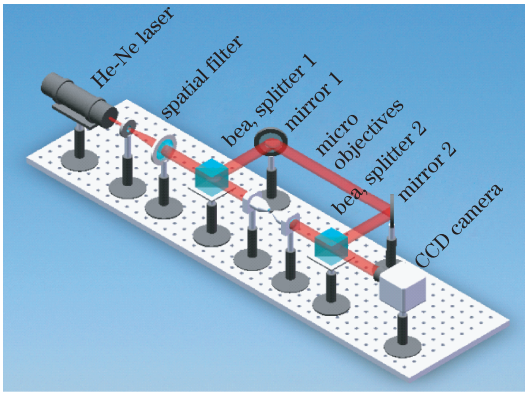

Fig. 5. Schematic setup of high speed QIM.

distributions with original phase are 0.9845 and 0.9274. Figures 4(d)−(g) shows the proposed phase unwrapping procedures with FFT method, and Figs. 4(h)−(k) shows the those procedures with HT method. The simulation phase retrieval results show that the method could deal with the condition with low noise. The *c.c.* of the results in Figs. 4(g) and (k) are 0.9833 and 0.9197, respectively, which are close to the results via traditional phase unwrapping algorithms. Moreover, we compare sections of RBCs in our simulation results as shown in Fig. 4(l) which shows retrieval results fit with the original setting phase well. However, with the increase of the noise, the accuracy of retrieving phase is decreasing. Through calculation, we have found if the signal-to-noise ratio (SNR) is less than ∼24.7 dB, the proposed phase unwrapping method with HT algorithm could not well find the phase jumping. While for FFT based method, it could suffer larger noises. However, if the SNR is less than ∼14.7 dB, the *c.c.* value will be less than 0.9. It is obvious that in the condition with noise, FFT method works better than HT method since HT method keeps details of the samples while keeps the information of noise. While, using FFT method, the first order extraction could filter much noises which fits for the proposed phase unwrapping method since low noise will appear in the final phase wrapped map. Thus, in the following experiment, FFT phase extraction method is combined with proposed phase unwrapping method in order to recover the quantitative distribution of the RBC.

In order to evaluate the performance of the proposed method, we consider experimental case. Interferogram of red blood cells have been acquired by a transmission interferometric microscope, base on a Mach–Zehnder configuration in Fig. 5. Linear polarized light from a 4-mW He-Ne laser (λ=632.8 nm, ϕ=0.7 mm, ZCN) after expanding ($M = f_2/f_1 = 8$) and collimating is split into two beams by a polarization-maintaining beam cube (China Daheng Group). The microscopic system composed by a pair of micro-objectives (25×, NA=0.4) is set in the sample arm. The samples (rabbit RBCs) are placed in thin slide-tape-slide chamber and put near the focal plane of the micro-objectives to achieve higher magnification. To achieve off-axis interferograms, the mirror in the reference arm is adjusted to make the reference beam tilting with respect to the sample beam. Another polarization-maintaining beam cube is used to combine both the sample beam and reference beam. The recording device adopts a CCD camera (Stingray F-146 B, AVT, Germang) with 1388×1038 pixels and 4.65×4.65 (μm) square pixel size. And it has an acquisition rate of 15 frames/s at the full resolution. It is noted that "high-speed" means short phase unwrapping time other than interferogram capturing time, which is not so important in this setup because only one interferogram is needed to recover the phase.

Mature RBCs represent a very particular type of structure; they lack nuclei and organelles and thus can be modeled as optically homogeneous objects. RBCs were attained by incubating erythrocytes suspensions derived from healthy rabbits not receiving any pharmacological treatment. Leukocytes and platelets were removed by the method of Beutler *et al.*[27]. The RBCs are cultured in NaCl solution with 0.9% mass fraction.

We used the fast phase unwrapping method proposed in this letter to recover the phase distribution of the RBC in Fig. 6. Figure 6(a) shows the interferogram and the DIC imaging (BX 51, Olympus, Japan) of rabbit RBC. From the DIC imaging, it is obvious that the RBCs present biconcave structures. Figure 6(b) is the wrapped phase distribution retrieved by FFT method, since it has better anti-noise capability than other methods. With traditional phase unwrapping method[21], unwrapped phase distribution could be obtained as shown in Fig. 6(c). Here we applied the fast phase unwrapping method, firstly, calculating the phase with FFT method

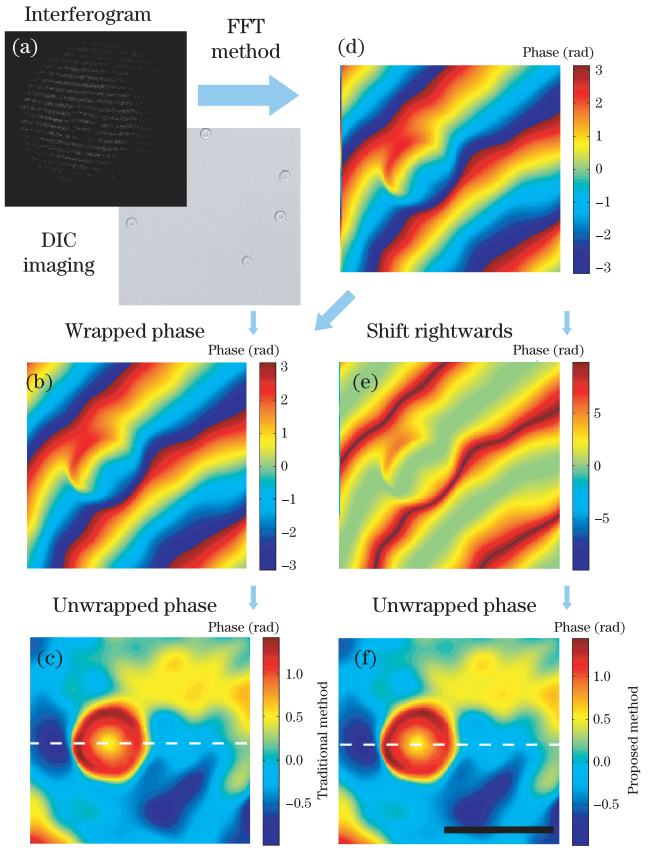

Fig. 6. Fast phase unwrapping algorithm for QIM experiment. (a) interferogram and the DIC imaging; (b) wrapped phase distribution retrieved by FFT method; (c) unwrapped phase distribution solved by Ref. [29]; (d) rightwards shifted wrapped phase; (e) multiplication of (b) and (d); (f) unwrapped phase distribution solved by proposed fast phase method. The black bar in (f) represents 10 μm.

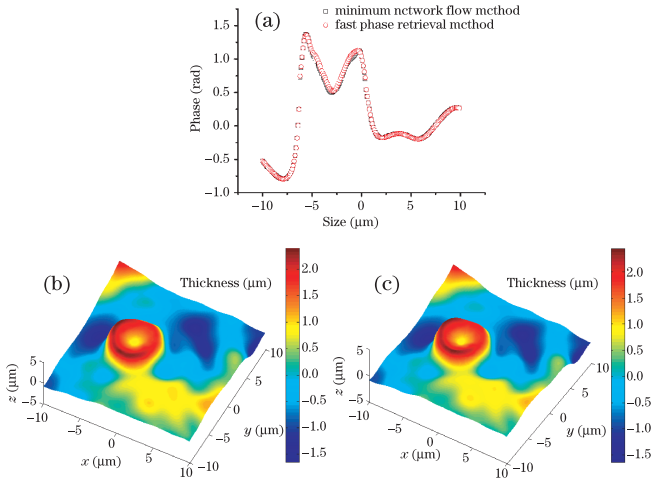

Fig. 7. (a) Phase distributions of RBC (white dotted lines in Figs. 6(c) and (f)); (b), (c) topographic figures of RBC obtained from traditional method and proposed method, respectively.

and then obtaining the rightwards one pixel shifted wrapped phase in Fig. 6(d). Figure 6(e) shows the multiplication of Figs. 6(b) and (d), the blue lines clearly indicate edges for adding step phases. The final unwrapped phase could be solved as seen in Fig. 6(f). From Figs. 6(c) and (f) which are unwrapped phase distributions with traditional method and proposed method, respectively, the biconcave structure is apparent and the diameter of RBC is ∼7.5 μm.

In order to compare the traditional phase unwrapping method and proposed fast phase unwrapping method, we have shown the phase distributions in the center of RBC (white dotted lines in Figs. 6(c) and (f)) obtained by these two methods in Fig. 7(a). The data of the proposed method fits well with traditional method which indicates that the fast phase retrieval method could be applied well in QIM. Assuming the refractive index of RBC is 1.40 and the 0.9% mass fraction NaCl solution's refractive index is 1.34, the structures of RBC could be revealed as Figs. 7(b) and (c) by different methods. The most thickness part of RBC is ∼2.5 μm and the thickness of center part is ∼1.0 μm which agrees well with the RBC model.

In conclusion, phase unwrapping plays an important role in QIM, which directly determines the accuracy and efficiency of the phase measuring. In this letter, we propose a fast phase unwrapping method for recovering quantitative phase distributions. This method is a rather simple technique to obtain continuous phase distribution from single interferogram without background information or dual wavelength interferogram capturing. The simulation clearly shows the accuracy of the proposed fast phase extraction method is high and calculating efficiency has been enhanced. With proposed method, it will be much easier to determine the phase discontinuities for its high contrast and wider range. The experimental results show that the new approach gives exactly the same result as the traditional approach while performing much faster. Based on this method, the high speed QIM could be applied to real time monitoring and detecting as well as large-scale phase distribution data analysis of biological samples.

This work was supported by the Priority Academic Program Development of Jiangsu Higher Education Institutions (PAPD), the National Natural Science Foundation of China (No. 31372399), and the Natural Science Foundation of Jiangsu Province (No. BK20130699) for Prof. Fei Liu. The authors thank Yanke Shan and Mingfei Xu in Single Molecule Nanometry Laboratory, Nanjing Agricultural University for their kindly help in the experiments and Dr. Haijiao Jiang in Nanjing Institute of Astronomical Optics and Technology, Chinese Academy of Sciences for his kind help and discussions.

References

1. J. Ma, C. Yuan, G. Situ, G. Pedrini, and W. Osten, Chin. Opt. Lett. **11,** 090901 (2013).
2. J. Zheng, B. Yao, R. A. Rupp, T. Ye, P. Gao, J. Min, and R. Guo, Chin. Opt. Lett. **10,** 010901 (2012).
3. W. Chen and X. Chen, Opt. Express **18,** 13536 (2010).
4. W. Chen and X. Chen, J. Opt. Soc. Am. A **29,** 585 (2012).
5. M. Mir, B. Bhaduri, R. Wang, R. Zhu, and G Popescu, Progress in Opt. **57,** 133 (2012).
6. H. Schreiber and J. Bruning, *Phase Shifting Interferometry* (Wiley, New York, 2007).
7. J. Vargas, J. A. Quiroga, and T. Belenguer, Opt. Lett. **36,** 1326 (2011).
8. J. Vargas, J. A. Quiroga, and T. Belenguer, Opt. Lett. **36,** 2215 (2011).
9. S. Wang, L. Xue, H. Li, J. Lai, Y. Song, and Z. Li, Appl. Phys. B (to be published).
10. M. Takeda, H. Ina, and S. Kobayashi, J. Opt. Soc. Am. **72,** 156 (1982).
11. L. Xue, S. Wang, K. Yan, N. Sun, P. Ferraro, Z. Li, and F. Liu, Opt. Commun. **316,** 5 (2014).
12. T. Ikeda, G. Popescu, R. R. Dasari, and M. S. Feld, Opt. Lett. **30,** 1165 (2005).
13. L. Xue, J. Lai, S. Wang, and Z. Li, Biomed. Opt. Express **2,** 987 (2011).
14. S. Wang, L. Xue, J. Lai, and Z. Li, Optik **124,** 1897 (2013).
15. S. Wang, L. Xue, J. Lai, Y. Song, and Z. Li, J. Opt. **15,** 075301 (2013).
16. S. Wang, N. Sun, L. Xue, H. Li, J. Lai, Y. Song, and Z. Li, Opt. Commun. **304,** 148 (2013).
17. M. Servin and F. Cuevas, J. Mod. Opt. **42,** 1853 (1995).
18. S. K. Debnath and Y. Park, Opt. Lett. **36,** 4677 (2011).
19. B. Bhaduri and G. Popescu, Opt. Lett. **37,** 1868 (2012).
20. D. Ghiglia and L. Romero, J. Opt. Soc. Am. A **11,** 107 (1994).
21. M. Costantini, IEEE Tran. on Geoscience and Remote Sensing **36,** 813 (1998).
22. J. Gass, A. Dakoff, and M. K. Kim, Opt. Lett. **28,** 1141 (2003).
23. H. Pham, C. Edwards, L. Goddard, and G. Popescu, Appl. Opt. **52,** A97 (2013).
24. H. S. Abdul-Rahman, M. A. Gdeisat, D. R. Burton, M. J. Lalor, F. Lilley, and C. J. Moore, Appl. Opt. **46,** 6623 (2007).
25. J. C. Estrada, J. Vargas, J. M. Flores-Moreno, and J. A. Quirog, Appl. Opt. **51,** 7549 (2012).
26. S. Tsinopoulos and D. Polyzos, Appl. Opt. **38,** 5499 (1999).
27. E. Beutler, C. West, and K. G. Blume, J. Lab. Clin. Med. **88,** 328 (1976).